6

High-Precision Frequency Measurement Using Digital Signal Processing

Ya Liu[1,2], Xiao Hui Li[1] and Wen Li Wang[1]
[1]National Time Service Center, Chinese Academy Sciences, Xi'an, Shaanxi
[2]Key Laboratory of Time and Frequency Primary Standard, Institute of National Time Service Center Chinese Academy of Sciences, Xi'an, Shaanxi
China

1. Introduction

High-precision frequency measurement techniques are important in any branch of science and technology such as radio astronomy, high-speed digital communications, and high-precision time synchronization. At present, the frequency stability of some of atomic oscillators is approximately 1E-16 at 1 second and there is no sufficient instrument to measure it (C. A. Greenhall, 2007).

Kinds of oscillator having been developed, some of them have excellent long-term stability when the others are extremely stable frequency sources in the short term. Since direct frequency measurement methods is far away from the requirement of measurement high-precision oscillator, so the research of indirect frequency measurement methods are widely developed. Presently, common methods of measuring frequency include Dual-Mixer Time Difference (DMTD), Frequency Difference Multiplication (FDM), and Beat-Frequency (BF). DMTD is arguably one of the most precise ways of measuring an ensemble of clocks all having the same nominal frequency, because it can cancel out common error in the overall measurement process (D. A. Howe & DAVID A & D.B.Sulliivan, 1981). FDM is one of the methods of high-precision measurement by multiplying frequency difference to intermediate frequency. Comparing with forenamed methods, the BF has an advantage that there is the simplest structure, and then it leads to the lowest device noise. However, the lowest device noise doesn't means the highest accuracy, because it sacrifices accuracy to acquire simple configuration. Therefore, the BF method wasn't paid enough attention to measure precise oscillators.

With studying the BF methods of measuring frequency, we conclude that the abilities of measuring frequency rest with accuracy of counter and noise floor of beat-frequency device. So designing a scheme that it can reduce circuit noise of beat-frequency device is mainly mission as the model of counter has been determined. As all well known, reducing circuit noise need higher techniques to realize, and it is hardly and slowly, therefore, we need to look for another solution to improve the accuracy of BF method. In view of this reason, we design a set of algorithm to smooth circuit noise of beat-frequency device and realize the DFSA design goal of low noise floor (Ya Liu, 2008).

This paper describes a study undertaken at the National Time Service Center (NTSC) of combining dual-mixer and digital cross-correlation methods. The aim is to acquire high short-term stability, low cost, high reliability measurement system. A description of a classical DMTD method is given in Section 2. Some of the tests of the cross-correlation algorithm using simulated data are discussed in Section 3.2. The design of DFSA including hardware and software is proposed in Section 3.3-3.4. In section 4 the DFSA is applied to measure NTSC's cesium signal and the results of noise floor of DFSA is given. Future possible modifications to the DFSA and conclusions are discussed in Section 4.

2. Principle of DMTD method

The basic idea of the Dual Mixer Time Difference Method (DMTD) dates back to 1966 but was introduced in "precision" frequency sources measurement some 10 years later (S. STEIN, 1983). The DMTD method relies upon the phase measurement of two incoming signals versus an auxiliary one, called common offset oscillator. Phase comparisons are performed by means of double-balance mixers. It is based on the principle that phase information is preserved in a mixing process. A block diagram is shown in figure 1.

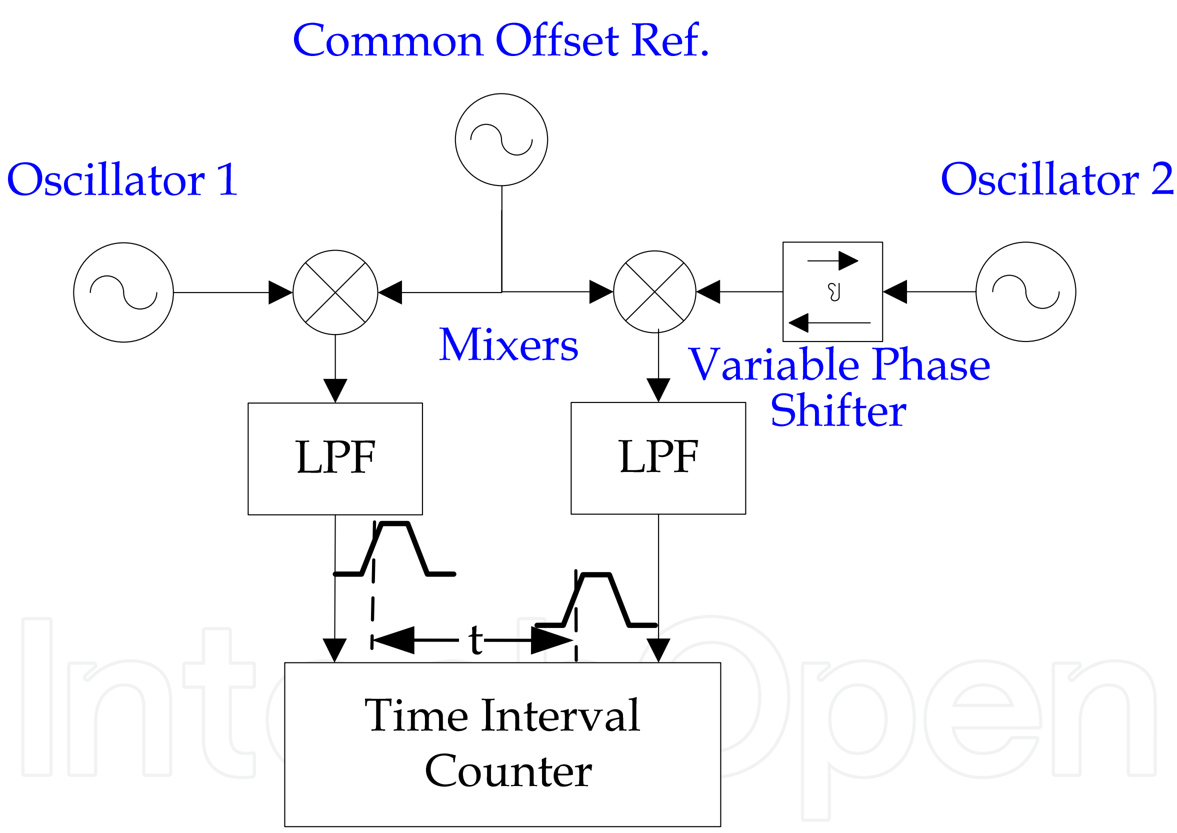

Fig. 1. Block diagram of a dual mixer time difference measuring system

DMTD combines the best features of Beat Method and Time Interval Counter Method, using a time interval counter to measure the relative phase of the beat signals. The measurement resolution is increased by the heterodyne factor (the ratio of the carrier to the beat frequency). For example, mixing a 10 MHz source against a 9.9999 MHz Hz offset reference will produce a 100 Hz beat signal whose period variations are enhanced by a factor of 10 MHz/100 Hz = 10^5. Thus, a period counter with 100 ns resolution (10 MHz clock) can resolve clock phase changes of 1 ps.

The DMTD setup is arguably the most precise way of measuring an ensemble of clocks all having the same nominal frequency. The usual idea thought that the noise of the common offset oscillator could be cancelled out in the overall measurement process. However, if the oscillator 1 and oscillator 2 are independent, then the beat signals of being fed into counter are not coherent. Figure 2 shows the beat signals that are fed into the time interval counter, thus, the beat signals of two test oscillators against the common offset oscillator are zero crossing at different sets of points on the time axis, such as t1 and t2. When time interval counter is used to measure the time difference of two beat signals, the time difference will be contaminated by short-term offset oscillator noise, here called common-source phase error (C. A. Greenhall, 2001, 2006). This DMTD method is inevitable common-source phase error when use counter to measure time difference. To remove the effect of common-source phase error need to propose other processing method.

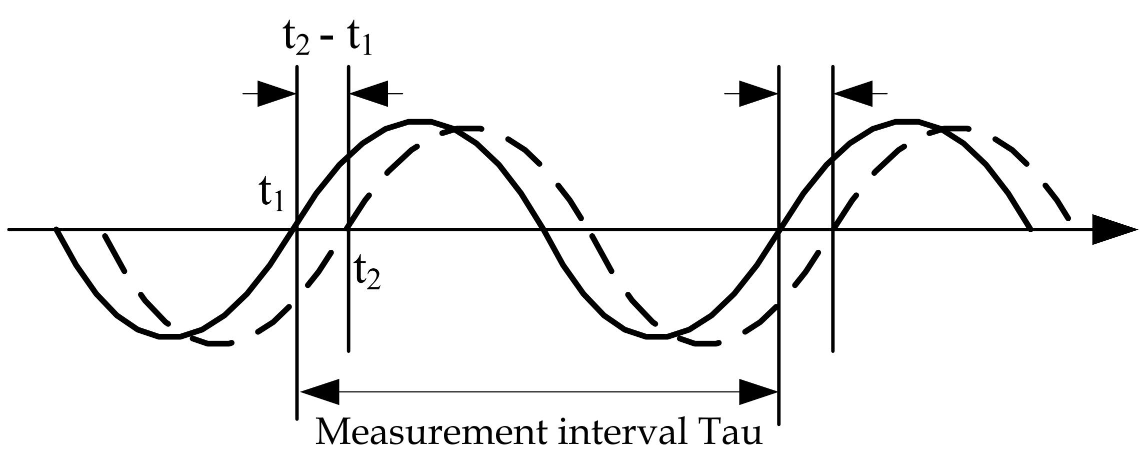

Fig. 2. Beat signals from double-balance mixers

3. Frequency measurement using digital signal processing

To remove the effect of common offset oscillator phase noise and improve the accuracy of measuring frequency, we proposed to make use of digital signal processing method measuring frequency. A Multi-Channel Digital Frequency Stability Analyzer has been developed in NTSC.

3.1 System configuration

This section will report on the Multi-Channel Digital Frequency Stability Analyzer (DFSA) based upon the reformed DMTD scheme working at 10MHz with 100Hz beat frequency. DFSA has eight parallel channels, and it can measure simultaneously seven oscillators. The block diagram of the DFSA that only includes two channels is reported in Fig. 3.

Common offset reference oscillator generates frequency signal, which has a constant frequency difference with reference oscillator. Reference oscillator and under test oscillator at the same nominal frequency are down-converted to beat signals of low frequency by mixing them with the common offset reference to beat frequency. A pair of analog-to-digital converters (ADC) simultaneously digitizes the beat signals output from the double-balance mixers. All sampling frequency of ADCs are droved by a reference oscillator to realize simultaneously sampling. The digital beat signals are fed into personal computer (PC) to computer the drift frequency or phase difference during measuring time interval.

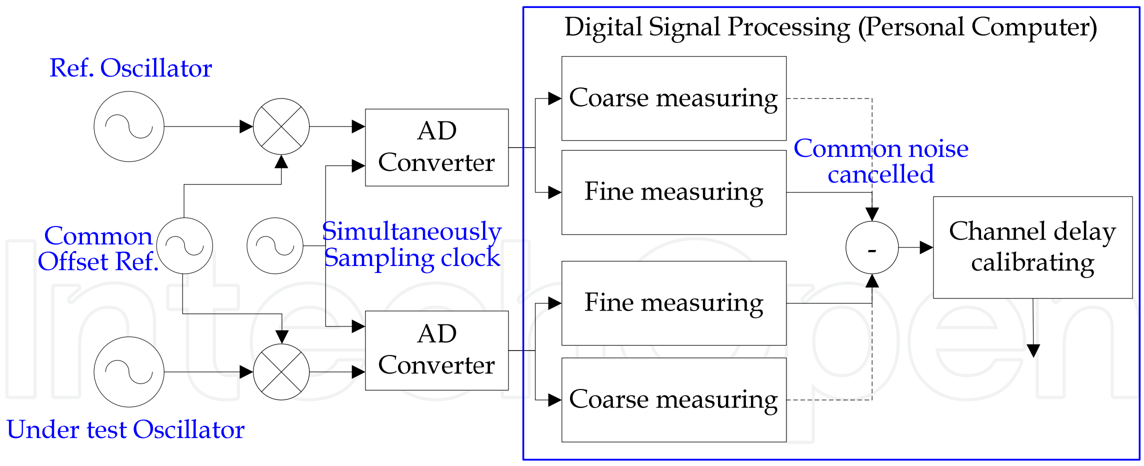

Fig. 3. Block diagram of the DFSA

3.2 Measurement methods

Digital beat signals processing is separated two steps that consist of coarse measuring and fine measuring. The two steps are parallel processed at every measurement period. The results of coarse measuring can be used to remove the integer ambiguity of fine measuring.

3.2.1 Coarse measurement

The coarse measurement of beat frequency is realized by analyzing the power spectrums beat signal. The auto power spectrums of the digital signals are calculated to find the frequency components of beat signal buried in a noisy time domain signal. Generating the auto power spectrum is by using a fast Fourier transform (FFT) method. The auto power spectrum is calculated as shown in the following formula:

$$S_x(f) = \frac{FFT(x)FFT^*(x)}{n^2} \tag{3.1}$$

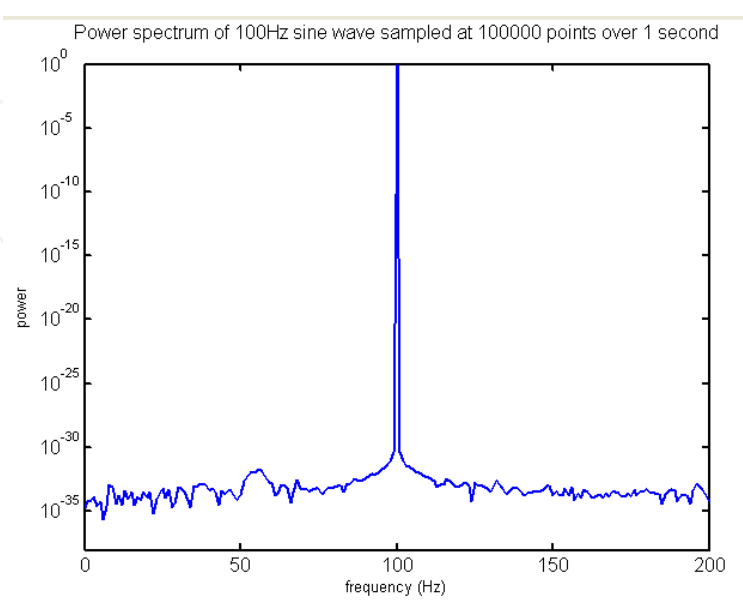

Fig. 4. The power vs. frequency in Hertz

Where x is the beat signals array; n is the number of points in the signal array x; * denotes a complex conjugate. According aforementioned formula, figure 4 plots power spectrum of a 100 Hz sine wave. As expected, we get a very strong peak at a frequency of 100 Hz. Therefore, we can acquire the frequency corresponding to the maximum power from the plot of auto power spectrum.

3.2.2 Fine measurement

The beat signals from the ADCs are fed into PC to realize fine measuring too. Fine measurement includes the cross-correlation and interpolation methods. To illuminate the cross-correlation method, figure 5 shows a group of simulation data. The simulation signals of 1.08Hz are digitized at the sampling frequency of 400Hz. The signal can be expressed by following formula.

$$x(n) = \sin(2\pi \frac{f}{f_s} n + \varphi_0) \tag{3.2}$$

Where f indicates the frequency of signal, the f_s is sampling frequency, n refers the number of sample, and φ_0 represents the initial phase. In the figure 5, the frequency of signal can be expressed:

$$f = f_N + \Delta f = (1 + 0.05)Hz \tag{3.3}$$

There the f_N refers the integer and Δf indicates decimal fraction. In addition, there is the initial phase $\varphi_0 = 0$ and $f_s = 400Hz$. There are sampled two seconds data in the figure 5, so we can divide it into data1 and data2 two groups. Data1 and data2 can be expressed respectively by following formulas:

$$x_1(n) = \sin(2\pi \frac{f_N + \Delta f}{f_s} n + \varphi_0), n \in [0,399] \tag{3.4}$$

$$\begin{aligned} x_2(n) &= \sin(2\pi \frac{f_N + \Delta f}{f_s} n + \varphi_0), n \in [400,799] \\ &= \sin(2\pi \frac{f_N + \Delta f}{f_s} n + \varphi_0 + 2\pi(f_N + \Delta f)), n \in [0,399] \end{aligned} \tag{3.5}$$

According the formula (3.5), the green line can be used to instead of the red one in the figure 5 to show the phase difference between data1 and data2. And then the phase difference is the result that the decimal frequency Δf of signal is less than 1Hz. Therefore, we can calculate the phase difference to get Δf. The cross-correlation method is used to calculate the phase difference of adjacent two groups data.

The cross-correlation function can be shown by following formula:

$$R_{x_1 x_2}(m) = \frac{1}{N} \sum_{n=0}^{N-1} x_1(n) x_2(n+m) = \frac{1}{2} \cos(2\pi \frac{f_N + \Delta f}{f_s} m + 2\pi(f_N + \Delta f)) \tag{3.6}$$

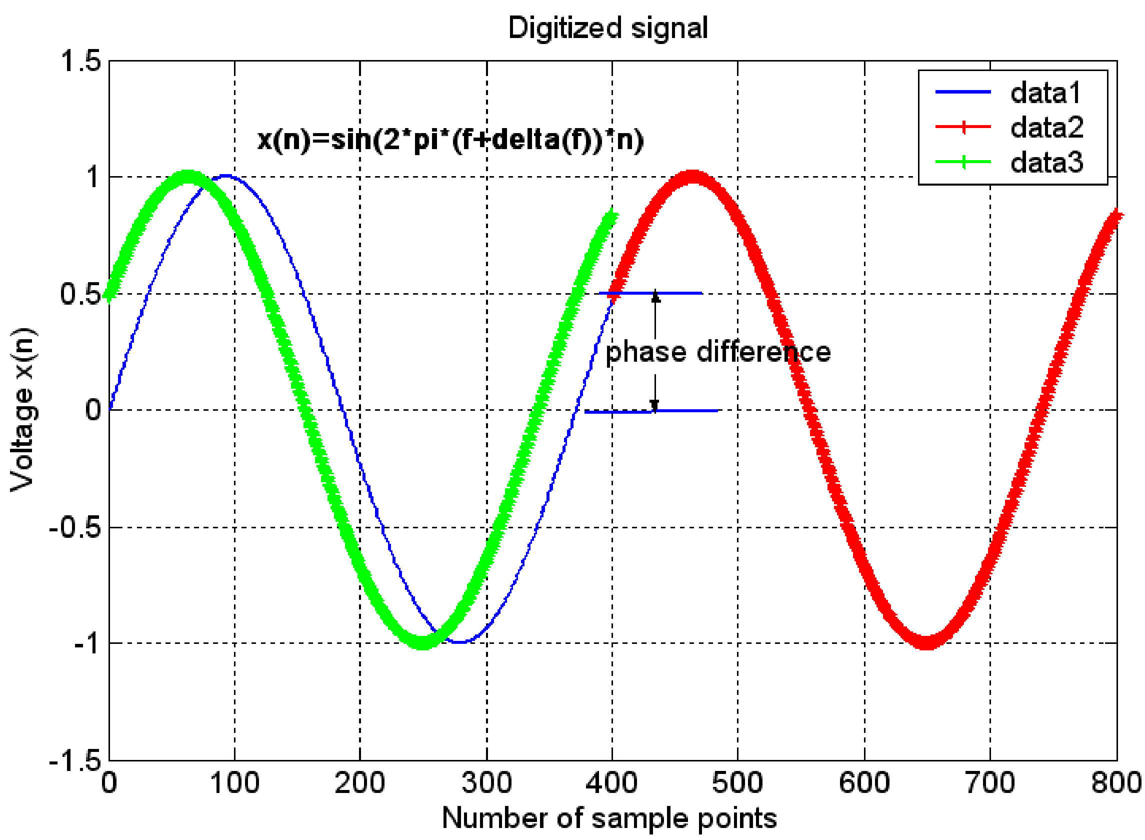

Fig. 5. Signals of 1.08Hz are digitized at the sampling frequency of 400Hz

Where m denotes the delay and m=0, 1, 2…N-1. To calculate the value of Δf , m is supposed to be zero. So we can get the formula (3.7):

$$R_{x_1x_2}(0) = \frac{1}{2}\cos(2\pi(f_N + \Delta f)) = \frac{1}{2}\cos(2\pi\Delta f)) \tag{3.7}$$

From the formula (3.7), the Δf that being mentioned in formula (3.3) means frequency drift of under test signal during the measurement interval can be acquired. On the other side, the f_N is measured by using the coarse measurement method. So combining coarse and fine measurement method, we can get the high-precision frequency of under test signals.

3.3 Hardware description

The Multi-Channel Digital Frequency Stability Analyzer consists of Multi-channel Beat-Frequency signal Generator (MBFG) and Digital Signal Processing (DSP) module. The multi-channel means seven test channels and one calibration channel with same physical structure. The system block diagram is shown in figure 6.

The MBFG is made up of Offset Generator (OG), Frequency Distribution Amplifier (FDA), and Mixer. There are eight input signals, and seven signals from under test sources when the other one is designed as the reference, generally the most reliable source to be chosen as reference. The reference signal f_0 is used to drive the OG. The OG is a special frequency synthesizer that can generate the frequency at $f_r = f_0 - f_b$. The output of OG drives FDA to acquire eight or more offset sources at frequency f_r. Seven under test signals, denoted frequency $f_{xi}, i = 1,2,3...$, are down-converted to sinusoidal beat-frequency signals at nominal frequency f_b by mixing them with the offset sources at frequency f_r. The signal flow graph is showed in figure 6.

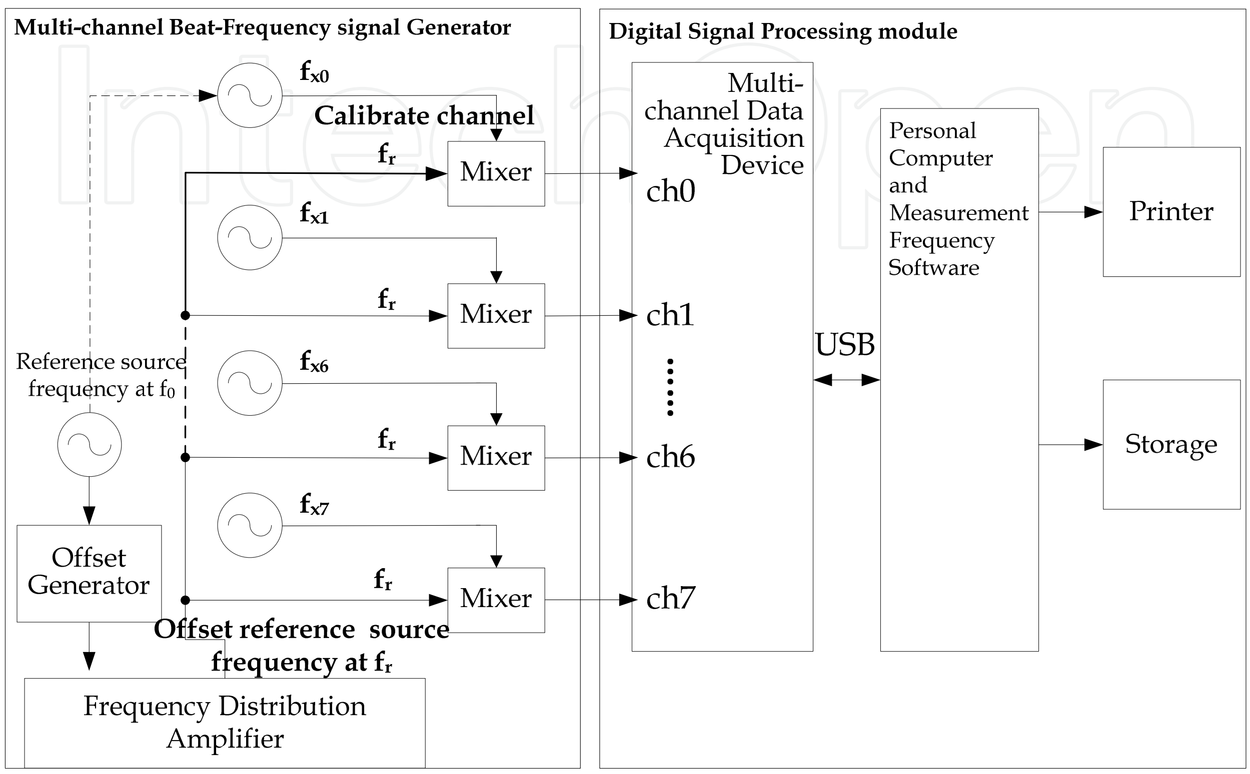

Fig. 6. Block Diagram of the Multi-Channel Digital Frequency Stability Analyzer

The channel zero is calibrating channel, which input the reference source running at frequency f_0 to test real time noise floor of the DFSA, and then can calibrate systematic errors of the other channels. The calibrating can be finished depending on the relativity between the input of channel zero and the output of OG. Because both signals come from one reference oscillator, they should have strong relativity that can cancel the effect of reference oscillator noise.

The Digital Signal Processing module consists of multi-channel Data Acquisition device (DAQ), personal computer (PC) and output devices. The Measurement Frequency (MF) software is installed in PC to analyze data from DAQ. The beat frequency signals, which are output from the MBFG that are connected to channels of analog-to-digital converter respectively, are digitized according to the same timing by the DAQ that are driven by a clock with sampling frequency N. Then, MF software retrieves the data from buffer of DAQ, maintains synchronization of the data stream, carries out processing of measurement (including frequency, phase difference, and analyzing stability), stores original data to disk, and manages the output devices.

The MBFG output must be sinusoidal beat frequency signals, because processing beat frequency signal make use of the property of trigonometric function. It has the obvious difference with traditional beat frequency method using square waveform and Zero Crosser Assembly.

3.4 Software description

The Measurement Frequency software (MF) of the Multi-Channel Digital Frequency Stability Analyzer is operated by the LabWindows/CVI applications. MF configures the parameters of DAQ, stores original data and results of measuring to disk, maintains synchronization of the data stream, carries out the algorithms of measuring frequency and phase difference, analyzes frequency stability, retrieves the stored data from disk and prepares plots of original data, frequency, phase difference, and Allan deviation. Figure 8 shows the main interface. To view interesting data, user can click corresponding control buttons to show beat signals graph, frequency values, phase difference and Allan deviation and so on.

MF consists of four applications, a virtual instrument panel that is the user interface to control the hardware and the others via DLL, a server program is used to manage data, processing program, and output program. Figure 7 shows the block diagram of MF software.

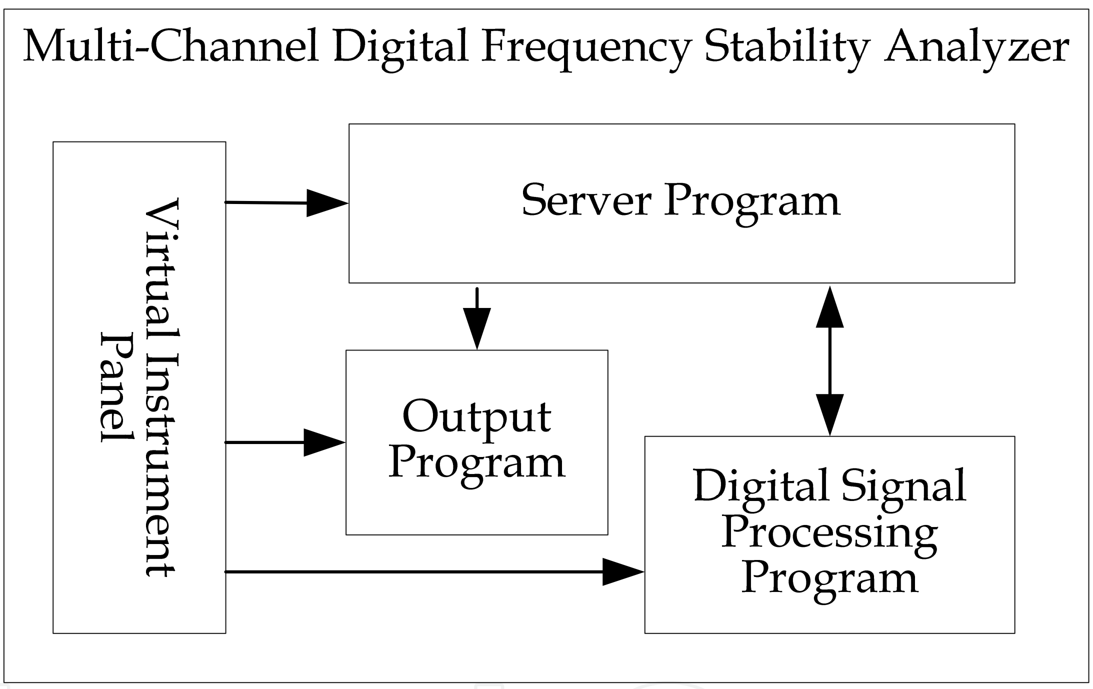

Fig. 7. Block Diagram of the Measurement Frequency Software

The virtual instrument panel have been developed what can be handled friendly by users. It looks like a real instrument. It consists of options pull-down menu, function buttons, choice menus. Figure 8 (a) shows the parameters setting child panel. Users can configure a set of parameters what involve DAQ, such as sampling frequency, amplitude value and time base of DAQ. Figure 8 (b) shows the screen shot of MF main interface. On the left of Fig. 8 (b), users can assign any measurement channel start or pause during measurement. On the right of Fig. 8 (b), strip chart is used to show the data of user interesting, such as real-time original data, measured frequency values, phase difference values and Allan deviation. To distinguish different curves, different coloured curves are used to represent different channels when every channel name has a specific colour. Figure 8 (c) shows the graph of the real-time results of frequency measurement when three channels are operated synchronously, and (d) shows the child panel what covers the original data, frequency values and Allan deviation information of one of channel.

Server program configures the parameters of each channel, maintains synchronization of the data stream, carries out the simple preprocessing (either ignore those points that are significantly less than or greater than the threshold or detect missing points and substitute extrapolated values to maintain data integrity), stores original data and results of measuring to disk.

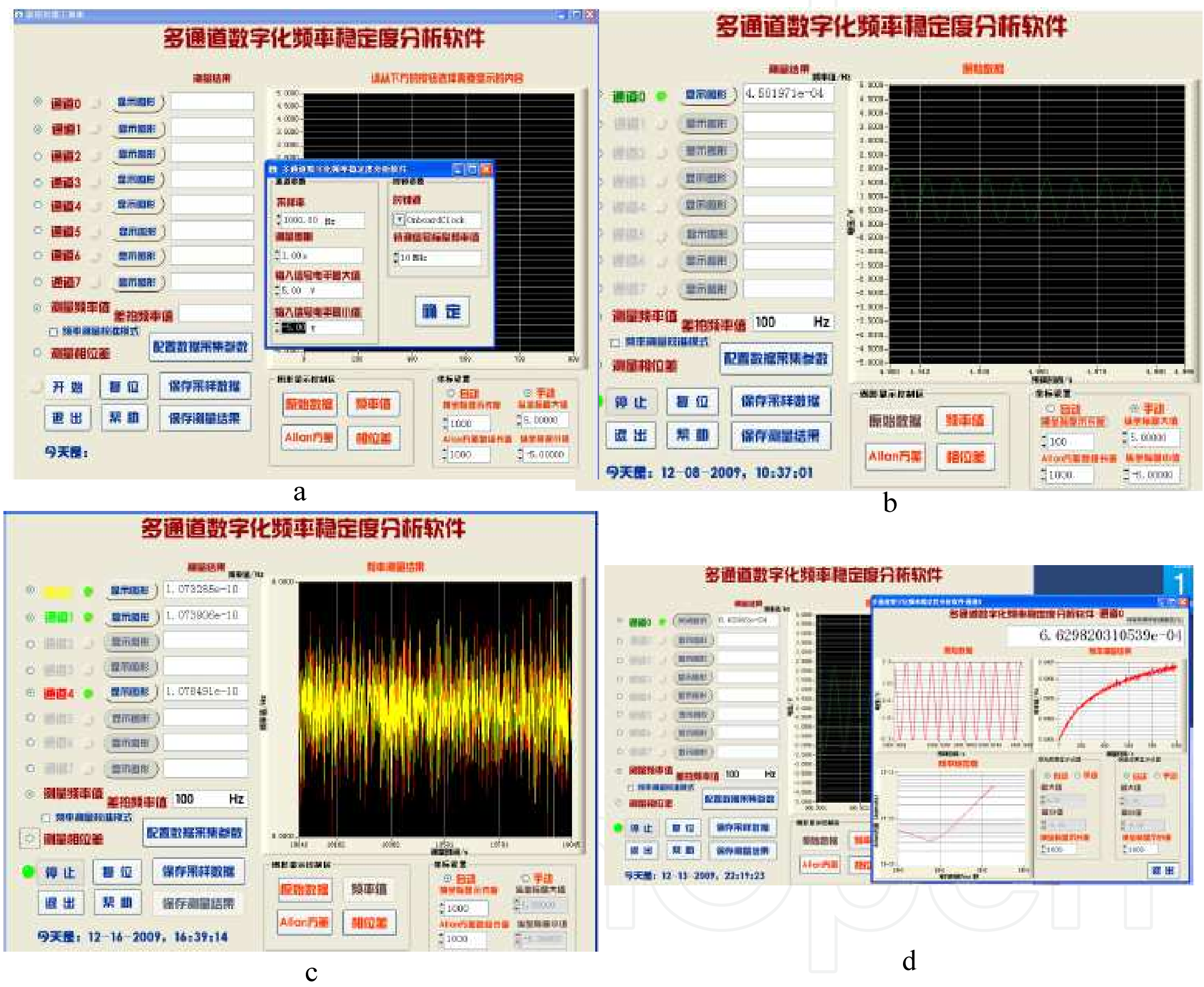

Fig. 8. MF software, (a) shows the window of configuring parameters and choosing channels, (b) shows the strip chart of real-time original data of one of channels, (c) shows the graph of the real-time results of frequency measurement, (d) shows the child panel that covers the original data, frequency values and Allan deviation information of one of channel.

Digital signal processing program retrieves the stored data from disk and carries out the processing. Frequency measurement includes dual-channel phase difference and single frequency measurement modes in the digital signal processing program. The program will run different functions according to the select mode of users. Single frequency measurement mode can acquire frequency values and the Allan deviation of every input signal source. In addition, the dual-channel phase difference mode can output the phase difference between two input signals.
The output program manages the interface that communicate with other instruments, exports the data of user interesting to disk or graph. Text files of these data are available if the user need to analyze data in the future.

3.5 Measurement precision

The dual-mixer and digital correlation algorithms are applied to DFSA. In this system, has symmetrical structure and simultaneously measurement to cancel out the noise of common offset reference source. (THOMAS E. PARKER, 2001) So the noise of common offset source can be ignored. The errors of the Multi-Channel Digital Frequency Stability Analyzer relate to thermal noise and quantization error (Ken Mochizuki, 2007 & Masaharu Uchino, 2004). The cross-correlation algorithm can reduce the effect of circuit noise floor and improve the measurement precision by averaging amount of sampling data during the measurement interval. In addition, this system is more reliability and maintainability because the structure of system is simpler than other high-precision frequency measurement system. This section will discuss the noise floor of the proposed system.
To evaluate the measurement precision of DFSA, we measured the frequency stability when the test signal and reference signal came from a single oscillator in phase (L.Sojdr, J. Cermak, 2003). Ideally, between the test channel and reference were operated symmetrically, so the error will be zero. However, since the beat signals output from MBFG include thermal noise, the error relate to white Gaussian noise with a mean value of zero.
Although random disturbance noise can be removed by running digital correlation algorithms in theory, we just have finite number of sampling data available in practice. So it will lead to the results that the cross-correlation between the signal and noise aren't completely uncorrelated. Then the effect of random noise and quantization noise can't be ignored. We will discuss the effect of ignored on measurement precision in following chapter.
According to above formula (3.7) introduction, the frequency drift Δf could be acquired by measuring the beat-frequency signal at frequency. But in the section 3.2.2, the beat signal is no noise, and that is inexistence in the real world. When the noises are added in the beat signal, it should be expressed like:

$$v_i(n) = V_i \sin(2\pi \frac{f_b + \Delta f_i}{N} n + \varphi_i) + g_i(n) + l_i(n), i = 1,2,3... \quad (3.8)$$

Where $v_i(n)$ represents beat-frequency signal, V_i indicates amplitude of channel i, f_b is the nominal frequency of beat-frequency signal, unknown frequency drift Δf_i of source under test in channel i, φ_i denotes the initial phase of channel i. Here N is sampling frequency of analog-to-digital converter (ADC), $g_i(n)$ denotes random noise of channel i, $l_i(n)$ is

quantization noise of channel i and generates by ADC, n is a positive integer and its value is in the range $1 \sim \infty$.
Formula (3.8) could be transformed into following normalized expression (3.9) to deduce conveniently.

$$v_i(n) = \sin(2\pi \frac{f_b + \Delta f_i}{N} n + \varphi_i) + g_i(n) + l_i(n) \tag{3.9}$$

To realize one time frequency measurement, sampling beat-frequency signal must be continuous operated at least two seconds. For example, the j-th measurement frequency of channel i will analyze the j second $v_{ij}(n)$ and j+1 second $v_{i(j+1)}(n)$ data from DAQ.
The cross-correlation between $v_{ij}(n)$ and $v_{i(j+1)}(n)$ have been used by following formula:

$$\begin{aligned} R_{ij}(m) &= \frac{1}{N}\sum_{n=0}^{N-1} v_{ij}(n)v_{i(j+1)}(n+m) \\ &= \frac{1}{N}\sum_{n=0}^{N-1}[x_{ij}(n) + g_{ij}(n) + l_{ij}(n)] \times [x_{i(j+1)}(n+m) + g_{i(j+1)}(n+m) + l_{i(j+1)}(n+m)] \\ &= \frac{1}{2}\cos(\omega_{ij}m + \Phi_{ij}) + R_{x_{ij}g_{i(j+1)}} + R_{x_{ij}l_{i(j+1)}} + R_{g_{ij}x_{i(j+1)}} + R_{g_{ij}g_{i(j+1)}} + R_{g_{ij}l_{i(j+1)}} + R_{l_{ij}x_{i(j+1)}} \\ &\quad + R_{l_{ij}g_{i(j+1)}} + R_{l_{ij}l_{i(j+1)}} \end{aligned} \tag{3.10}$$

Formula (3.10) could be split into three parts; with the first part is cross-correlation function between signals $x(n)$:

$$A = \frac{1}{2}\cos(\omega_{ij}m + \Phi_{ij}) \tag{3.11}$$

the second part is the cross-correlation function between noise and signal;

$$B = R_{x_{ij}g_{i(j+1)}} + R_{x_{ij}l_{i(j+1)}} + R_{g_{ij}x_{i(j+1)}} + R_{l_{ij}x_{i(j+1)}} \tag{3.12}$$

the third part is the cross-correlation function between noise and noise:

$$C = R_{g_{ij}g_{i(j+1)}} + R_{g_{ij}l_{i(j+1)}} + R_{l_{ij}g_{i(j+1)}} + R_{l_{ij}l_{i(j+1)}} \tag{3.13}$$

According to the property of correlation function, if two circular signals are correlated then it will result in a period signal with the same period as the original signal. Therefore, the C can be denoted average $R_{ij}(m)$ over m:

$$C = \frac{1}{N}\sum_{m=0}^{N-1} R_{ij}(m) \tag{3.14}$$

The term $B = R_{x_{ij}g_{i(j+1)}} + R_{x_{ij}l_{i(j+1)}} + R_{g_{ij}x_{i(j+1)}} + R_{l_{ij}x_{i(j+1)}}$ of cross-correlation can't be ignored. Because the term B isn't strictly zero. We will discuss the effect of ignoring B and C on measurement precision in following section.

According to the property of cross-correlation and sine function, we have

$$
\begin{aligned}
&R_{x_{ij}g_{i(j+1)}}(m) = R_{g_{i(j+1)}x_{ij}}(-m) = \frac{1}{N}\sum_{n=0}^{N-1} g_{i(j+1)}(n)x_{ij}(n-m) \\
&= \frac{1}{N}\sum_{n=0}^{N-1} g_{i(j+1)}(n)\sin(\varphi_{ij} + \omega_{ij}n - \omega_{ij}m) \\
&= \frac{1}{N}\sum_{n=0}^{N-1} g_{i(j+1)}(n)[\sin(\varphi_{ij} + \omega_{ij}n)\cos(\omega_{ij}m) - \cos(\varphi_{ij} + \omega_{ij}n)\sin(\omega_{ij}m)] \\
&= \frac{1}{N}\cos(\omega_{ij}m)\sum_{n=0}^{N-1} g_{i(j+1)}(n)\sin(\varphi_{ij} + \omega_{ij}n) - \frac{1}{N}\sin(\omega_{ij}m)\sum_{n=0}^{N-1} g_{i(j+1)}(n)\cos(\varphi_{ij} + \omega_{ij}n)
\end{aligned}
\tag{3.15}
$$

Similarly, for other cross-correlation, we have

$$
\begin{aligned}
&R_{x_{ij}l_{i(j+1)}}(m) = \frac{1}{N}\sum_{n=0}^{N-1} l_{i(j+1)}(n)x_{ij}(n-m) \\
&= \frac{1}{N}\cos(\omega_{ij}m)\sum_{n=0}^{N-1} l_{i(j+1)}(n)\sin(\varphi_{ij} + \omega_{ij}n) - \frac{1}{N}\sin(\omega_{ij}m)\sum_{n=0}^{N-1} l_{i(j+1)}(n)\cos(\varphi_{ij} + \omega_{ij}n)
\end{aligned}
\tag{3.16}
$$

$$
\begin{aligned}
&R_{g_{ij}x_{i(j+1)}}(m) = \frac{1}{N}\sum_{n=0}^{N-1} g_{ij}(n)x_{i(j+1)}(n+m) \\
&= \frac{1}{N}\cos(\omega_{ij}m)\sum_{n=0}^{N-1} g_{ij}(n)\sin(\varphi_{i(j+1)} + \omega_{ij}n) + \frac{1}{N}\sin(\omega_{ij}m)\sum_{n=0}^{N-1} g_{ij}(n)\cos(\varphi_{i(j+1)} + \omega_{ij}n)
\end{aligned}
\tag{3.17}
$$

$$
\begin{aligned}
&R_{l_{ij}x_{i(j+1)}}(m) = \frac{1}{N}\sum_{n=0}^{N-1} l_{ij}(n)x_{i(j+1)}(n+m) \\
&= \frac{1}{N}\cos(\omega_{ij}m)\sum_{n=0}^{N-1} l_{ij}(n)\sin(\varphi_{i(j+1)} + \omega_{ij}n) + \frac{1}{N}\sin(\omega_{ij}m)\sum_{n=0}^{N-1} l_{ij}(n)\cos(\varphi_{i(j+1)} + \omega_{ij}n)
\end{aligned}
\tag{3.18}
$$

Then, the B can be obtained as follows:

$$
\begin{aligned}
B = &\frac{1}{N}\cos(\omega_{ij}m)[\sum_{n=0}^{N-1} g_{i(j+1)}(n)\sin(\varphi_{ij} + \omega_{ij}n) + \sum_{n=0}^{N-1} l_{i(j+1)}(n)\sin(\varphi_{ij} + \omega_{ij}n) \\
&+ \sum_{n=0}^{f_s-1} g_{ij}(n)\sin(\varphi_{i(j+1)} + \omega_{ij}n) + \sum_{n=0}^{f_s-1} l_{ij}(n)\sin(\varphi_{i(j+1)} + \omega_{ij}n)] \\
&+ \frac{1}{N}\sin(\omega_{ij}m)[\sum_{n=0}^{N-1} g_{ij}(n)\cos(\varphi_{i(j+1)} + \omega_{ij}n) - \sum_{n=0}^{N-1} g_{i(j+1)}(n)\cos(\varphi_{ij} + \omega_{ij}n) \\
&+ \sum_{n=0}^{N-1} l_{ij}(n)\cos(\varphi_{i(j+1)} + \omega_{ij}n) - \sum_{n=0}^{N-1} l_{i(j+1)}(n)\cos(\varphi_{ij} + \omega_{ij}n)]
\end{aligned}
\tag{3.19}
$$

The sum of formula (3.19) is equal to zero in the range [0,N-1].

$$\sum_{m=0}^{N-1} B = 0 \tag{3.20}$$

In view of the Eq. (3.20), although the B isn't strictly zero, their sum is equal to zero. We all known that on the right-hand side of Eq.(3.14) is the sum of cross-correlation function. Applying the Eq. (3.20) to (3.14) term by term, we obtain that the Eq.(3.14) strictly hold. Now we have the knowledge that the term C doesn't effect on the measurement results and we just need to discuss the term B as follows. Eq. (3.12) can be given by

$$R_{ij}(0) - \frac{1}{N}\sum_{m=0}^{N-1} R_{ij}(m) = \frac{1}{2}\cos(\Phi_{ij}) + B \tag{3.21}$$

Let the error terms that are caused by the white Gaussian noise and the quantization noise be represented by $B_1 = R_{x_{ij}g_{i(j+1)}} + R_{g_{ij}x_{i(j+1)}}$ and $B_2 = R_{x_{ij}l_{i(j+1)}} + R_{l_{ij}x_{i(j+1)}}$ respectively. So B can be expressed by $B = B_1 + B_2$.

Here, quantization noise is generally caused by the nonlinear transmission of AD converter. To analysis the noise, AD conversion usual is regarded as a nonlinear mapping from the continuous amplitude to quantization amplitude. The error that is caused by the nonlinear mapping can be calculated by using either the random statistical approach or nonlinear determinate approach. The random statistical approach means that the results of AD conversion are expressed with the sum of sampling amplitude and random noise, and it is the major approach to calculate the error at present.

We assume that $g(t)$ is Gaussian random variable of mean '0'and standard deviation 'σ_g^2'. In the view of Eq.(3.15) and (3.17), we have obtained the standard deviation as follow:

$$\sigma_{B_1}^2 = \frac{2\sigma_g^2}{N} \tag{3.22}$$

Assume that the AD converter is round-off uniformly quantizer and using quantization step Δ . Then $l(t)$ is uniformly distributed in the range $\pm\Delta/2$ and its mean value is zero and standard deviation is $(\Delta^2/12)$. We have

$$\sigma_{B_2}^2 = \frac{2\Delta^2}{12N} \tag{3.23}$$

For B_1 and B_2 are uncorrelated, then

$$\sigma_B^2 = \sigma_{B_1}^2 + \sigma_{B_2}^2 = \frac{2\sigma_g^2}{N} + \frac{2\Delta^2}{12N} \tag{3.24}$$

The mean square value of $\frac{1}{2}\cos(\Phi_{ij}) + B$ on the right-hand side of formula (3.21) will be calculated by the following formula to evaluate the influence of noise on measurement initial phase difference.

$$\begin{aligned}
&\frac{1}{N}\sum_{m=0}^{N-1}(\frac{1}{4}\cos^2(\Phi_{ij})+B\cos(\Phi_{ij})+B^2) \\
&=\frac{1}{4}\cos^2(\Phi_{ij})+\frac{1}{N}\sum_{m=0}^{N-1}(B\cos(\Phi_{ij})+B^2) \\
&=\frac{1}{4}\cos^2(\Phi_{ij})+(\frac{2\sigma_g^2}{N}+\frac{2\Delta^2}{12N})+\frac{1}{N}\sum_{m=0}^{N-1}B\cos(\Phi_{ij}) \\
&\le\frac{1}{4}\cos^2(\Phi_{ij})+(\frac{2\sigma_g^2}{N}+\frac{2\Delta^2}{12N})+\frac{1}{N}\sum_{m=0}^{N-1}B \\
&=\frac{1}{4}\cos^2(\Phi_{ij})+(\frac{2\sigma_g^2}{N}+\frac{2\Delta^2}{12N})
\end{aligned} \tag{3.25}$$

Where σ_g^2 represent standard deviation of Gaussian random variable, Signal Noise Ratio $SN=\frac{V^2}{\sigma_g^2}$, and here the V is the amplitude of input signal, let amplitude resolution of a-bit digitize and quantization step be Δ, here variable 'a' can be 8~24. We have $\frac{\Delta}{V}=\frac{2}{2^a-1}$ (Ken Mochizuki, 2007). Applying this equation to formula (3.25) term by term, we obtain

$$\sigma_e=\sqrt{\frac{1}{4}\cos^2(\Phi_{ij})+\frac{1}{N}(\frac{2V^2}{SN^2}+\frac{2\Delta^2}{12})} \tag{3.26}$$

Where σ_e is the standard deviation of measurement initial phase difference. The standard deviation of digital correlation algorithms depends on the sampling frequency N, SNR and amplitude resolution 'a', as understood from formula (3.26). Here the noise of amplitude resolution can be ignored if the 'a' is sufficiently bigger than 16-bit and the SNR is smaller than 100 dB. The measurement accuracy for this method is mostly related to SNR of signal. This method has been tested that has the strong anti-disturbance capability.

4. System noise floor and conclusion

To evaluate the noise floor, we designed the platform when the test signal and reference signal were distributed in phase from a single signal generator. The signal generator at 10MHz and the beat-frequency value of 100Hz were set. For this example obtained the Allan deviation (square root of the Allan variance (DAVID A, HOWE)) of $\sigma_y(\tau)=4.69E-14$ at $\tau=1$ second and $\sigma_y(\tau)=1.27E-15$ at $\tau=1000$ second.

The measurement ability could be optimized further by improving the performance of OG. Because the reference of the system is drove by the output of OG.

Since the digital correlation techniques can smooth the effects of random disturbance of the MBFG, it can achieve higher measurement accuracy than other methods even if on the same MBFG.

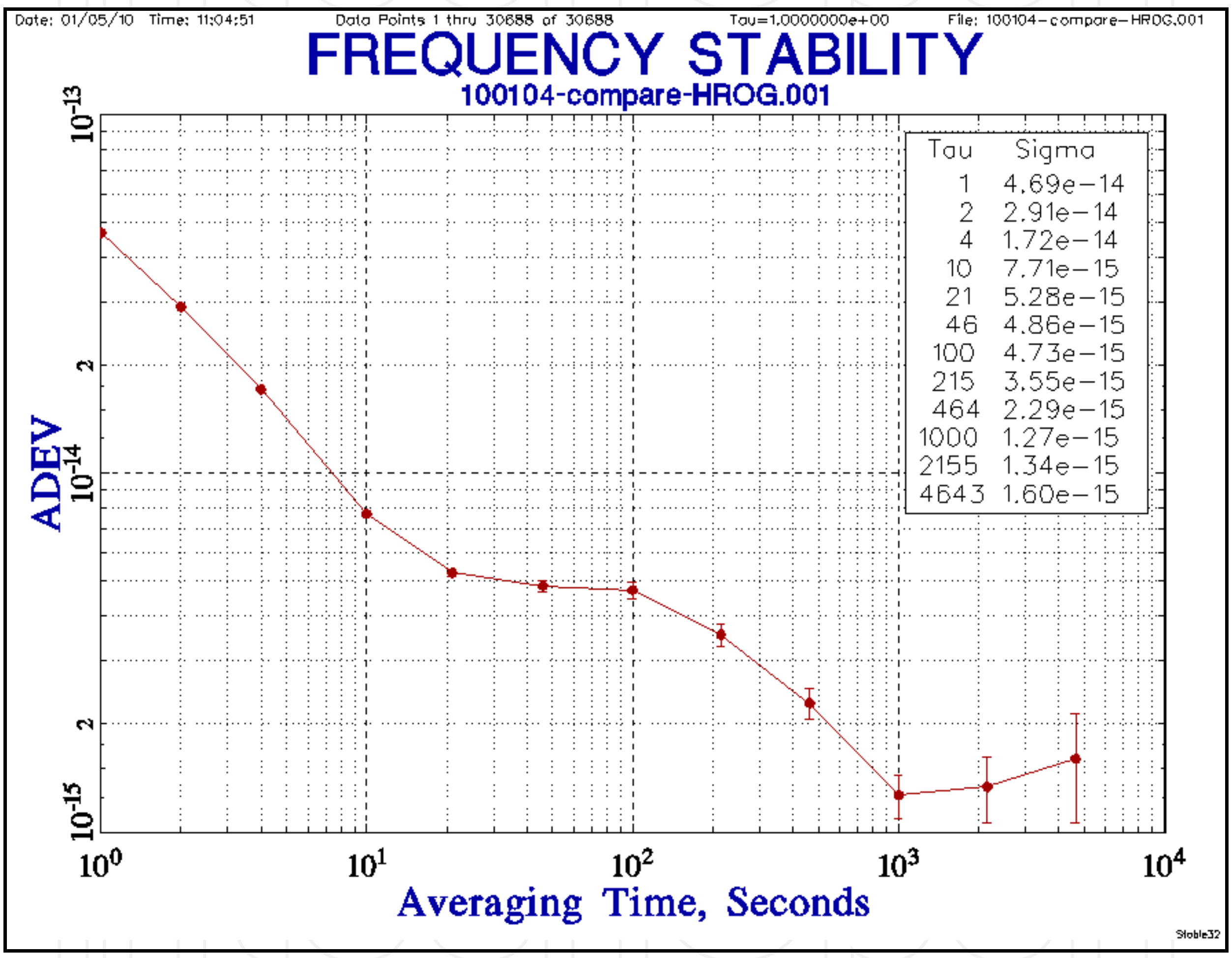

Fig. 9. An example of noise floor characteristics of the DFSA: Allan deviation

Additional, the design of calibration channel that is proposed to remove the systematic error is useful to acquire better performance for current application. A comprehensive set of noise floor tests under all conditions has not been carried out with the current system.

The system hardware consists only of MBFG, DAQ and PC. Compared with the conventional systems using counter and beat-frequency device, the system can be miniaturized and moved conveniently. As expected, system noise floor is good enough for current test requirement. The system will take measurement of wide range frequency into account in the future. Intuitive operator interface and command remotely will be design in following work.

5. Acknowledgment

The authors thank Bian Yujing and Wang Danni for instructing. I would like to thank the present of the Chinese Academy of sciences scholarship and Zhu Liyuehua Scholarship for the supporting. The work has been supported by the key program of West Light Foundation of The CAS under Grant 2007YB03 and the National Nature Science Funds 61001076 and 11033004.

6. References

Allan, D. W. – Daams, H.: *Picosecond Time Difference Measurement System* Proc. 29th Annual Symposium Frequency Control, Atlantic City, USA, 1975, 404–411.

C. A. Greenhall, A. Kirk, and G. L. Stevens, 2002, *A multi-channel dual-mixer stability analyzer: progress report,* in Proceedings of the 33rd Annual Precise Time and Time Interval (PTTI) Systems and Applications Meeting, 27-29 November 2001, Long Beach, California, USA, pp. 377-383.

C. A. Greenhall, A. Kirk, and R. L. Tjoelker. *A Multi-Channel Stability Analyzer for Frequency Standards in the Deep Space Network*. 38th Annual Precise Time and Time Interval (PTTI) Meeting.2006.105-115

C. A. Greenhall, A. Kirk, R. L. Tjoelker. *Frequency Standards Stability Analyzer for the Deep Space Network*. IPN Progress Report.2007.1-12

D. A. Howe, D. W. Allan, and J. A. Barnes, 1981, *Properties of signal sources and measurement methods,* in Proceedings of the 35th Annual Frequency Control Symposium, 27-29 May 1961, Philadelphia, Pennsylvania, USA (Electronic Industries Association, Washington, D.C.), 1–47

D.A.Howe,C.A.Greenhall.Total Variance: a Progress Report on a New Frequency Stabbility Characterization.1999.

David A, Howe. *Frequency Stability*.1703-1720, National Institute of Standards and Technology (NIST)

D.B.Sulliivan, D.W.Allan, D.A.Howe and F.L.Walls, *Characterization of Clocks and Oscillators*, NIST Technical Note 1337.

E. A. Burt, D. G. Enzer, R. T. Wang, W. A. Diener, and R. L. Tjoelker, 2006, *Sub-10-16 Frequency Stability for Continuously Running Clocks: JPL's Multipole LITS Frequency Standard*s, in Proceedings of the 38th Annual Precise Time and Time Interval (PTTI)

Systems and Applications Meeting, 5-7 December 2006, Reston, Virginia, USA (U.S. Naval Observatory, Washington, D.C.), 271-292.

G. Brida, *High resolution frequency stability measurement system*, Review of Scientific Instruments, Vol., 73, NO. 5 May 2002, pp. 2171–2174.

J. Laufl M Calhoun, W. Diener, J. Gonzalez, A. Kirk, P. Kuhnle, B. Tucker, C. Kirby, R. Tjoelker. *Clocks and Timing in the NASA Deep Space Network*. 2005 Joint IEEE International Frequency Control Symposium and Precise Time and Time Interval (PTTI) Systems and Applications Meeting.2005.

Julian C. Breidenthal, Charles A. Greenhall, Robert L. Hamell, Paul F. Kuhnle. *The Deep Space Network Stability Analyzer*. The 26th Annual Precise Time and Time Interval (PTTI) Applications and Planning Meeting .1995.221-233

Ken Mochizuki, Masaharu Uchino, Takao Morikawa, *Frequency-Stability Measurement System Using High-Speed ADCs and Digital Signal Processing*, IEEE Transactions on Instrument, And Measurement, VOL. 56, NO. 5, Oct. 2007, pp. 1887–1893

L.Sojdr, J. Cermak, and G. Brida, *Comparison of High-Precision Frequency-Stability Measurement Systems*, Proceedings of the 2003 IEEE International Frequency Control Symposium, vol. A247, pp. 317–325, Sep. 2003

Masaharu Uchino, Ken Mochizuki, *Frequency Stability Measuring Technique Using Digital Signal Processing*, Electronics and Communications in Japan, Part 1, Vol. 87, No. 1, 2004, pp.21–33.

Richard Percival,Clive Green.*The Frequency Difference Between Two very Accurate and Stable Frequency Singnals*. 31st PTTI meeting.1999

R.T.Wang, M.D.Calhoun, A.Kirt, W. A. Diener, G. J. Dick, R.L. Tjoelker. *A High Performance Frequency Standard and Distribution System for Cassini Ka-Band Experiment.* 2005 Joint IEEE International Frequency Control Symposium (FCS) and Precise Time and Time Interval (PTTI) Systems and Applications Meeting.2005.919-924

S. Stein, D. Glaze, J. Levine, J. Gray, D. Hilliard, D. Howe, L. A. Erb, *Automated High-Accuracy Phase Measurement System. IEEE Transactions on Instrumentation and Measurement*. 1983.227-231

S. R. Stein, 1985, *Frequency and time their measurement and characterization*, in E. A. Gerber and A. Ballato, eds., Precision Frequency Control, Vol. 2 (Academic Press, New York), pp. 191–232, 399–416.

Thomas E. Parker. *Comparing High Performance Frequency Standards*. Frequency Control Symposium and PDA Exhibition, 2001. Proceedings of the 2001 IEEE International .2001.89-95

W. J. Riley, *Techniques for Frequency Stability Analysis*, IEEE International Frequency Control Symposium Tutorial Tampa, FL, May 4, 2003.

Ya Liu, Xiao-hui Li, Wen-Li Wang, Dan-Ni Wang, *Research and Realization of Portable High-Precision Frequency Set*, Computer Measurement & Control, vol.16, NO.1, 2008, pp21-23.

Ya Liu, Li Xiao-hui, Zhang Hui-jun, *Analysis and Comparison of Performance of Frequency Standard Measurement Systems Based on Beat-Frequency Method*, 2008 IEEE Frequency Control Symposium, 479-483

Ya Liu, Xiao-Hui Li, Yu-Lan Wang, *Multi-Channel Beat-Frequency Digital Measurement System for Frequency Standard*, 2009 IEEE International Frequency Control Symposium, 679-684

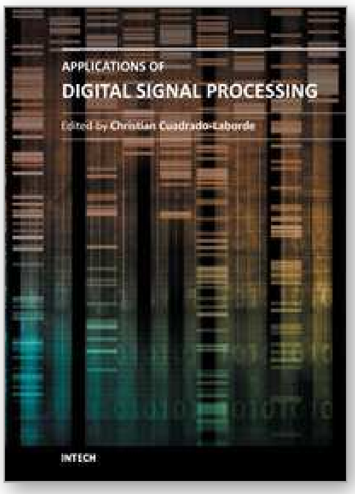

Applications of Digital Signal Processing
Edited by Dr. Christian Cuadrado-Laborde

ISBN 978-953-307-406-1
Hard cover, 400 pages
Publisher InTech
Published online 23, November, 2011
Published in print edition November, 2011

In this book the reader will find a collection of chapters authored/co-authored by a large number of experts around the world, covering the broad field of digital signal processing. This book intends to provide highlights of the current research in the digital signal processing area, showing the recent advances in this field. This work is mainly destined to researchers in the digital signal processing and related areas but it is also accessible to anyone with a scientific background desiring to have an up-to-date overview of this domain. Each chapter is self-contained and can be read independently of the others. These nineteenth chapters present methodological advances and recent applications of digital signal processing in various domains as communications, filtering, medicine, astronomy, and image processing.

How to reference
In order to correctly reference this scholarly work, feel free to copy and paste the following:

Ya Liu, Xiao Hui Li and Wen Li Wang (2011). High-Precision Frequency Measurement Using Digital Signal Processing, Applications of Digital Signal Processing, Dr. Christian Cuadrado-Laborde (Ed.), ISBN: 978-953-307-406-1, InTech, Available from: http://www.intechopen.com/books/applications-of-digital-signal-processing/high-precision-frequency-measurement-using-digital-signal-processing

INTECH
open science | open minds

InTech Europe
University Campus STeP Ri
Slavka Krautzeka 83/A
51000 Rijeka, Croatia
Phone: +385 (51) 770 447
Fax: +385 (51) 686 166
www.intechopen.com

InTech China
Unit 405, Office Block, Hotel Equatorial Shanghai
No.65, Yan An Road (West), Shanghai, 200040, China
中国上海市延安西路65号上海国际贵都大饭店办公楼405单元
Phone: +86-21-62489820
Fax: +86-21-62489821